Oral Oncology 69 (2017) 46–55

Contents lists available at ScienceDirect

Oral Oncology

journal homepage: www.elsevier.com/locate/oraloncology

Establishment and characterization of a clear cell odontogenic carcinoma cell line with *EWSR1-ATF1* fusion gene

Satoko Kujiraoka [a], Takaaki Tsunematsu [a], Yukiko Sato [b], Maki Yoshida [c], Ayataka Ishikawa [d], Rei Tohyama [e], Michio Tanaka [f], Yutaka Kobayashi [g], Tomoyuki Kondo [a], Aya Ushio [a], Kunihiro Otsuka [a], Mie Kurosawa [a], Masako Saito [a], Akiko Yamada [a], Rieko Arakaki [a], Hirokazu Nagai [h], Hiromasa Nikai [i], Kengo Takeuchi [b], Toshitaka Nagao [c], Youji Miyamoto [h], Naozumi Ishimaru [a,*], Yasusei Kudo [a,*]

[a] Department of Oral Molecular Pathology, Tokushima University Graduate School of Biomedical Sciences, Tokushima, Japan
[b] Department of Pathology, Cancer Institute, Japanese Foundation of Cancer Research, Tokyo, Japan
[c] Department of Human Pathology, Tokyo Medical University, Tokyo, Japan
[d] Department of Pathology, Saitama Cancer Center, Saitama, Japan
[e] Department of Clinical Laboratory, Tokyo Medical and Dental University, Dental Hospital, Tokyo, Japan
[f] Department of Pathology, Tokyo Metropolitan Hiroo Hospital, Tokyo, Japan
[g] Department of Oral Surgery, Tokyo Metropolitan Hiroo Hospital, Tokyo, Japan
[h] Department of Oral Surgery, Tokushima University Graduate School of Biomedical Sciences, Tokushima, Japan
[i] Department of Oral Maxillofacial Pathobiology, Hiroshima University Graduate School of Biomedical Sciences, Hiroshima, Japan

ARTICLE INFO

Article history:
Received 20 January 2017
Received in revised form 10 March 2017
Accepted 5 April 2017
Available online 10 April 2017

Keywords:
Clear cell odontogenic carcinoma
Malignant odontogenic tumor
Hyalinizing clear cell carcinoma
EWSR1-ATF1 fusion genes

ABSTRACT

Objective: Clear cell odontogenic carcinoma (CCOC) is a rare malignant odontogenic tumor (MOT) characterized by sheets and lobules of vacuolated and clear cells. To understand the biology of CCOC, we established a new cell line, CCOC-T, with *EWSR1-ATF1* fusion gene from a mandible tumor with distant metastasis and characterized this cell line.
Materials and methods: To detect the *EWSR1-ATF1* fusion gene, we used three CCOC cases, including the present case, by RT-PCR and FISH analysis. We characterized established CCOC-T cells by checking cell growth, invasion and the expression of odontogenic factors and bone-related factors. Moreover, the gene expression profile of CCOC-T cells was examined by microarray analysis.
Results: Histologically, the primary tumor was comprised of cords and nests containing clear and squamoid cells separated by fibrous septa. In addition, ameloblastomatous islands with palisaded peripheral cells were observed, indicating probable odontogenic origin. This tumor expressed the fusion gene *EWSR1-ATF1*, which underlies the etiology of hyalinizing clear cell carcinoma (HCCC) and potentially that of CCOC. We found a breakpoint in the *EWSR1-ATF1* fusion to be the same as that reported in HCCC. Established CCOC-T cells grew extremely slowly, but the cells showed highly invasive activity. Moreover, CCOC-T cells expressed bone-related molecules, odontogenic factors, and epithelial mesenchymal transition (EMT)-related molecules.
Conclusion: To the best of our knowledge, this is the first report on the establishment of a CCOC cell line. CCOC-T cells serve as a useful *in vitro* model for understanding the pathogenesis and nature of MOT.

Introduction

A malignant odontogenic tumor (MOT) is a rare tumor that comprises up to 2.1% of all odontogenic tumors [1]. Among them, clear cell odontogenic carcinoma (CCOC) is quite a rare MOT. To date, 81 cases have been reported in the literature [2–14]. Histologically, CCOC commonly shows a biphasic tumor pattern consisting of large sheets of clear epithelial cells and irregular cords of basaloid cells with scant eosinophilic cytoplasm, supported by a fibrous stroma [15]. As clear cell areas are frequently seen in other oral neoplasms, it is important to rule out these neoplasms of the oral and maxillofacial regions to obtain a correct diagnosis.

Recently, Bilodeau et al. identified an *EWSR1* rearrangement in five out of six CCOC cases, with confirmation of *ATF1* involvement in one case [16,17]. In addition, a case of CCOC with *EWSR1* and *ATF1* rearrangement has been reported [11]. However, the break-

* Corresponding authors.
E-mail addresses: ishimaru.n@tokushima-u.ac.jp (N. Ishimaru), yasusei@tokushima-u.ac.jp (Y. Kudo).

http://dx.doi.org/10.1016/j.oraloncology.2017.04.003
1368-8375/

point of *EWSR1-ATF1* fusion has not been clarified in CCOC. Hyalinizing clear-cell carcinoma (HCCC) is the first epithelial neoplasm shown to be associated with *EWSR1-ATF1* fusion [18]. HCCC is a rare minor salivary gland carcinoma composed of clear cells forming cords and nests in a hyalinized stroma [19]. As CCOC and HCCC have extensive morphologic and immunohistochemical overlap [20], these two types of tumor are difficult to distinguish histologically despite a difference in cell origin and location. These findings suggest that either CCOC represents an intraosseous HCCC or that CCOC represents an "odontogenic analogue" to HCCC.

To know the biology and pathogenesis of CCOC, we established a CCOC cell line with *EWSR1-ATF1* fusion and characterized this cell line.

Materials and methods

Tissue samples

A tissue sample obtained from a CCOC of a 64-year-old Japanese woman was used for generating a cell line. This study was approved by the Ethic Committee of Tokushima University (#1924) and was performed in compliance with the Declaration of Helsinki. At the time of tissue sampling, we informed the patient of the use of the tissues for future research and the patient complied. Informed consent was obtained verbally.

To detect the *EWSR1-ATF1* fusion gene, we used three CCOC cases including the present case (obtained from Tokushima University Hospital and Tokyo Metropolitan Hiroo Hospital), one HCCC case (obtained from Tokyo Medical University Hospital) and one oral squamous cell carcinoma (OSCC) case (obtained from Tokushima University Hospital). Formalin-fixed paraffin-embedded (FFPE) samples were used after obtaining approval from the ethics committee of each institution. Informed consent from all patients was obtained both verbally, as well as written, through a signature from all patients in this study.

Immunohistochemistry (IHC)

For the IHC analysis of original tumor tissues, paraffin-embedded sections were deparaffinized and subsequently applied to heat-induced antigen retrieval in 10 mM citrate buffer (pH 6.0). The sections were incubated with primary antibody, subsequently developed using horseradish peroxidase conjugated anti-rabbit immunoglobulin (Vector Laboratories), and counterstained with hematoxylin. The antibodies used in this study are listed in Supplementary Table 1.

Fluorescence in situ hybridization (FISH)

FISH analysis of fusion genes was performed with DNA probes for *EWSR1* and *ATF1*. Unstained sections (4 μm thick) were subjected to hybridization with the *EWSR1* break-apart probe kit (Vysis LSI *EWSR1* dual-color, break-apart rearrangement probe; Abbott Molecular) with bacterial artificial chromosome clone-derived probes for *ATF1* (CTD-2174I21). Hybridized slides were then stained with DAPI and examined using a BX51 fluorescence microscope (Olympus).

RT-PCR

Total RNA was obtained from FFPE samples using NucleoSpin® total RNA FFPE (Macherey-Nagel) and from the cultured cells using RNeasy Mini kits (Qiagen). The cDNA was synthesized from 1 μg total RNA using a PrimeScript RT reagent kit (Takara Bio). The primers used for RT-PCR analysis are listed in Supplementary Table 2. For detecting *EWSR1-ATF1* fusion gene, aliquots of the total cDNA were amplified with Tks Gflex™ DNA Polymerase (Takara Bio), and amplification was performed in a T100™ thermal cycler (Bio-rad) for 40 cycles following an initial denaturation at 98 °C for 10 s and 62 °C for 30 s. For conventional RT-PCR, aliquots of the total cDNA were amplified with Go Taq® Green Master Mix (Promega), and amplification was performed in a T100™ thermal cycler for 35 cycles after an initial denaturation at 95 °C for 30 s, an annealing at 60 °C for 30 s, and an extension at 72 °C for 1 min.

Cell culture

The tissue sample obtained from a CCOC was cut into small pieces and placed into 90-mm dishes (Falcon) with DMEM (Sigma-Aldrich) containing 10% fetal bovine serum (FBS) (Gibco). When these outgrowth cultures formed a confluent monolayer, the cells were subcultured after enzymatic removal with 0.05% trypsin-EDTA for the first passage. Then, we subcultured the cells for over 100 passages and used for the following analyses. A mucoepidermoid carcinoma (MEC) cell line, NCI-H292, was purchased from American Type Culture Collection and maintained in RPMI-1640 (Sigma-Aldrich) supplemented with 10% FBS. The OSCC cell line, HOC313, and an immortalized odontogenic epithelial cell line, iOdE, were maintained in DMEM supplemented with 10% FBS. The immortalized ameloblastoma cell line, AM-1, and the immortalized gingival epithelial cell line, OBA-9, were maintained in Keratinocyte-SFM (Invitrogen).

Cytogenetic analysis

Chromosomes were stained with Hoechst 33258. Images were captured using the Axio Imager 2 (Zeiss). The karyotypes of at least eight well-banded metaphases were analyzed.

Electron microscopic analysis

The cells were fixed with 2% of paraformaldehyde and 2% glutaraldehyde (GA) in 0.1 M phosphate buffer (PB) pH 7.4. Then, they were fixed with 2% GA in 0.1 M PB at 4 °C overnight. After fixation, the samples were postfixed in 2% osmium tetroxide with 0.1 M PB at 4 °C for 1 h. The samples were then dehydrated in graded ethanol solutions. Then, the samples were transferred to a resin (Quetol-812, Nisshin EM Co., Tokyo, Japan) and polymerized at 60 °C for 48 h. The polymerized resins were ultra-thin sectioned at 70 nm with a diamond knife using an ultramicrotome and the sections were mounted on copper grids. The ultrathin sections were double-stained with uranyal acetate and lead citrate. The grids were observed by a transmission electron microscope (JEM-1400Plus, JEOL Ltd., Tokyo, Japan) at an acceleration voltage of 80 kV. Digital images (2048 × 2048 pixels) were taken with a CCD camera (VELETA, Olympus Soft Imaging Solutions GmbH, Münster, Germany).

Xenograft

CCOC-T cells (1×10^6) were resuspended in 50 μL of Cellmatrix type I-A (Nitta Gelatin, Osaka, Japan), which is an acid-soluble collagen isolated from the tendon of a pig. Cells were injected subcutaneously into multiple sites of male SCID mice (CREA Japan Inc., Tokyo, Japan). This study was conducted in accordance with the "Fundamental Guidelines for the Proper Conduct of Animal Experiments and Related Activities in Academic Research Institutions" under the jurisdiction of the Ministry of Education, Culture, Sports, Science and Technology of the Japanese Government. This study's protocol was approved by the Committee on Animal Experiments at Tokushima University (#15011). The animals were monitored

for the formation of a tumor mass every week and were sacrificed two months later.

In vitro invasion assay

Invasiveness was assessed by an invasion assay using a 24-well cell culture insert with 8 μm pores (Falcon). The filter was coated with 20 μg of Matrigel (Becton Dickinson), a reconstituted basement membrane substance. The lower compartment contained 0.5 mL of medium. Following trypsinization, 1.2×10^5 cells were resuspended in 100 μL of DMEM supplemented with 10% FBS and placed in the upper compartment of the cell culture insert for 23 h. At the end of the incubation, the cells were fixed with methanol and stained with hematoxylin. The cells on the upper surface of the filter were removed by wiping with a cotton swab and the invasiveness of the cells was determined by counting via a light microscope at 100× magnification. We performed the assay three times and three fields were randomly selected for counting for each assay.

Microarray analysis

The total RNA from the CCOC-T and NCI-H292 cells was isolated using an RNeasy Mini kit (Qiagen). The RNA quality was first checked for chemical purity using a NanoDrop spectrophotometer and then assessed for RNA integrity using the Bioanalyzer 2100 (Agilent Technologies). The total RNA (100 ng) was amplified and labeled using the Affymetrix Whole-Transcript (WT) Sense Target Labeling Protocol, and the labeled RNA was hybridized to a GeneChip Human Gene 2.0 ST Array (Affymetrix). Gene expression data for the iOdE and OBA-9 cells was previously obtained [29]. Data visualization and analysis was performed using GeneSpring GX (Version 12.1) software. The accession number for the microarray dataset reported in this paper is GSE84300.

Results

CCOC case

A 64-year-old Japanese woman was referred for oral surgery for a radiolucent lesion. Panoramic radiography revealed an irregular-shaped and partially well-defined radiolucent lesion ranging from the lower left cuspid to the right retromolar region (Fig. 1A). A CT scan revealed an osteolytic lesion with a moth-eaten appearance combined with the disappearance of cortical bone (Fig. 1B). Fluorodeoxyglucose (^{18}F)-PET (FDG-PET) showed abnormal uptake at the sixth right rib and pubis. With a provisional diagnosis of MOT, surgical resection of the mandiblular tumor was performed. The gross examination of the resected specimen revealed a white tissue mass (Fig. 1C). After surgery, treatment was completed with chemotherapy. For the metastatic lesion of the rib and pubis, radiation therapy was performed. However, approximately one year after the surgery, other metastatic lesions were found in the left clavicle and right scapula.

Histology of CCOC case

The microscopic examination of this case revealed an epithelial tumor in the mandible consisting of small and irregular sheets or cords of neoplastic cells separated by dense collagenous stroma (Fig. 1D and E). The tumor islands were primarily composed of clear and squamoid cells (Fig. 1D and E). The clear cells contained various amounts of diastase-digestable PAS-positive granules and showed no positivity for alcian blue, indicating the glycogen content of the cytoplasm (Supplementary Table 3). In some areas, the tumor cells formed a tubular pattern (Fig. 1F). Moreover, the tumor cells were round to polygonal, had a clear cytoplasm, and exhibited cellular atypism. The IHC analysis showed that the tumor cells expressed cytokeratin AE1/AE3, p63, and CK-19 (Fig. 2A–C). As the differential diagnosis of a jaw tumor with clear cells, CCOC, intraosseous salivary gland tumors (e.g., MEC, epithelial-myoepithelial carcinoma, myoepithelial carcinoma, and HCCC), melanotic tumors, metastatic renal cell carcinoma and the clear-cell variant of calcifying epithelial odontogenic tumor were raised [21–24]. Tumor cells were negative for S100, vimentin, EMA, GFAP, αSMA, HMB-45, UCHL-1, CD10 and CD31 (Supplementary Table 3) and did not contain amyloid and mucus-producing cells (data not shown), indicating that the above-mentioned tumors, except for CCOC and HCCC, were ruled out. As CCOC and HCCC exhibit a morphologic and immunophenotypic overlap [24,25], it was difficult to distinguish CCOC and intraosseous HCCC. In this tumor, however, odontogenic features, such as the presence of ameloblastomatous islands with palisaded peripheral cells and the positivity of CK-19, were observed (Fig. 2C and D). Finally, this tumor was diagnosed as CCOC.

In this tumor, the Ki-67 labeling index was over 30% (Fig. 2E). Furthermore, neural invasion and necrosis were also observed (Fig. 2F). Clinically there was metastasis to the sixth right rib, pubis, left clavicle, and right scapula (Fig. 2G). These findings indicated a high degree of malignancy. Interestingly, this tumor strongly expressed EGFR, which can be a useful target of anticancer therapy (Fig. 2H).

EWSR1-ATF1 fusion gene in cases of CCOC

We performed two-color FISH for *EWSR1*, and *ATF1* genes in our case. Our case showed rearrangement of both *EWSR1* and *ATF1* genes (Fig. 3A). Then, we confirmed *EWSR1-ATF1* fusion transcripts by RT-PCR from an FFPE sample of this tumor (Fig. 3B). The direct sequence of the *EWSR1-ATF1* fusion transcript revealed that exon 11 of *EWSR1* was fused to exon 3 of *ATF1* (Fig. 3B), indicating that the breakpoint is the same as that found in HCCC [18]. Moreover, we examined the detection of *EWSR1-ATF1* fusion transcripts by RT-PCR from FFPE samples of two other CCOC cases (Case #1 and #2). An OSCC case (Case #4) was used as a negative control. Information and histology regarding the cases used in this experiment is presented in Fig. 3C, Supplementary Tables 4 and 5. The *EWSR1-ATF1* fusion transcript was detected in all two CCOC cases (Fig. 3B). As expected, the *EWSR1-ATF1* fusion transcript was also detected in the HCCC case (Case #3), but not in the OSCC case. Interestingly, we found that Case #1–3 had the same breakpoint of the *EWSR1-ATF1* fusion transcript as observed in our case (Fig. 3D and Supplementary Table 4).

Establishment of a CCOC cell line

CCOC-T cells were established from the above-mentioned CCOC case. We subcultured the cells to over P100. CCOC-T cells were spontaneously immortalized through bypassing senescence without any treatment and exhibited a polygonal shape (Fig. 4A). We performed a cytogenetic analysis by specifically examining the conventional karyotype of this cell line. The karyotypes of the CCOC-T cells were 50, XX, +5, +6, +8, +9, der(9;15)(q10;q10), del (12)(p12), −13, −16, +add(16)(q24)x2, −22, +mar1, and +mar2 (Fig. 4B). Among twenty cells examined in this analysis, the number of chromosomes was between 48 and 50 (Fig. 4C).

Upon EM examination of the CCOC-T cells, the tumor cells exhibited features of squamous cell differentiation, such as desmosomes with the insertion of tonofilaments (Fig. 4D). Moreover, the tumor cells demonstrated features of ductal cell differentiation, such as microvilli formation and intercellular or

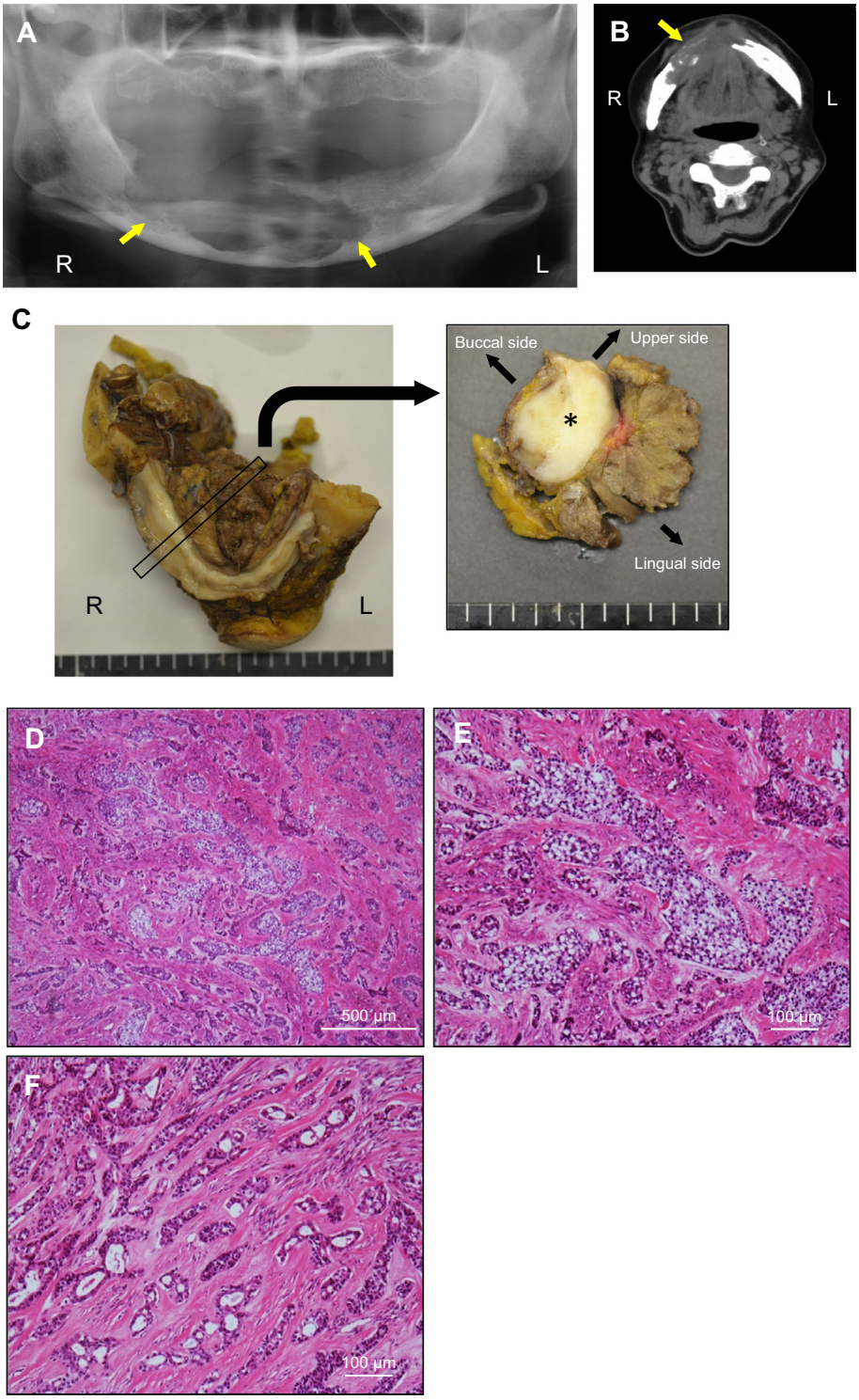

Fig. 1. A CCOC case. (A) A panoramic radiograph showing the radiolucent lesion (arrows). (B) CT scan image showing the radiolucent lesion (arrows). (C) The macroscopic finding of the resected specimen. A section of the mandible showing white soft tissue mass (asterisk). R: right, L: left. (D) The tumor consists of small and irregular sheets or cords of neoplastic cells separated by dense collagenous stroma. (E) Tumor islands are mainly composed of clear cells and squamoid cells. (F) The tumor cells partially form a tubular pattern.

intracytoplasmic lumina formation (Fig. 4E and F). Taken together, these findings are consistent with the histological features in the primary tumor.

CCOC-T cells were then injected subcutaneously with collagen gel into SCID mice to determine the level of tumor formation *in vivo*. After 2 month, tumor was observed, but size was small. The tumor nests were composed of both squamoid and clear cells (Fig. 4G). Tumor cells expressed p63, but not S100 (Supplementary Fig. S1). This result indicates that the tumors formed by the CCOC-T cells were histologically similar to the primary tumor.

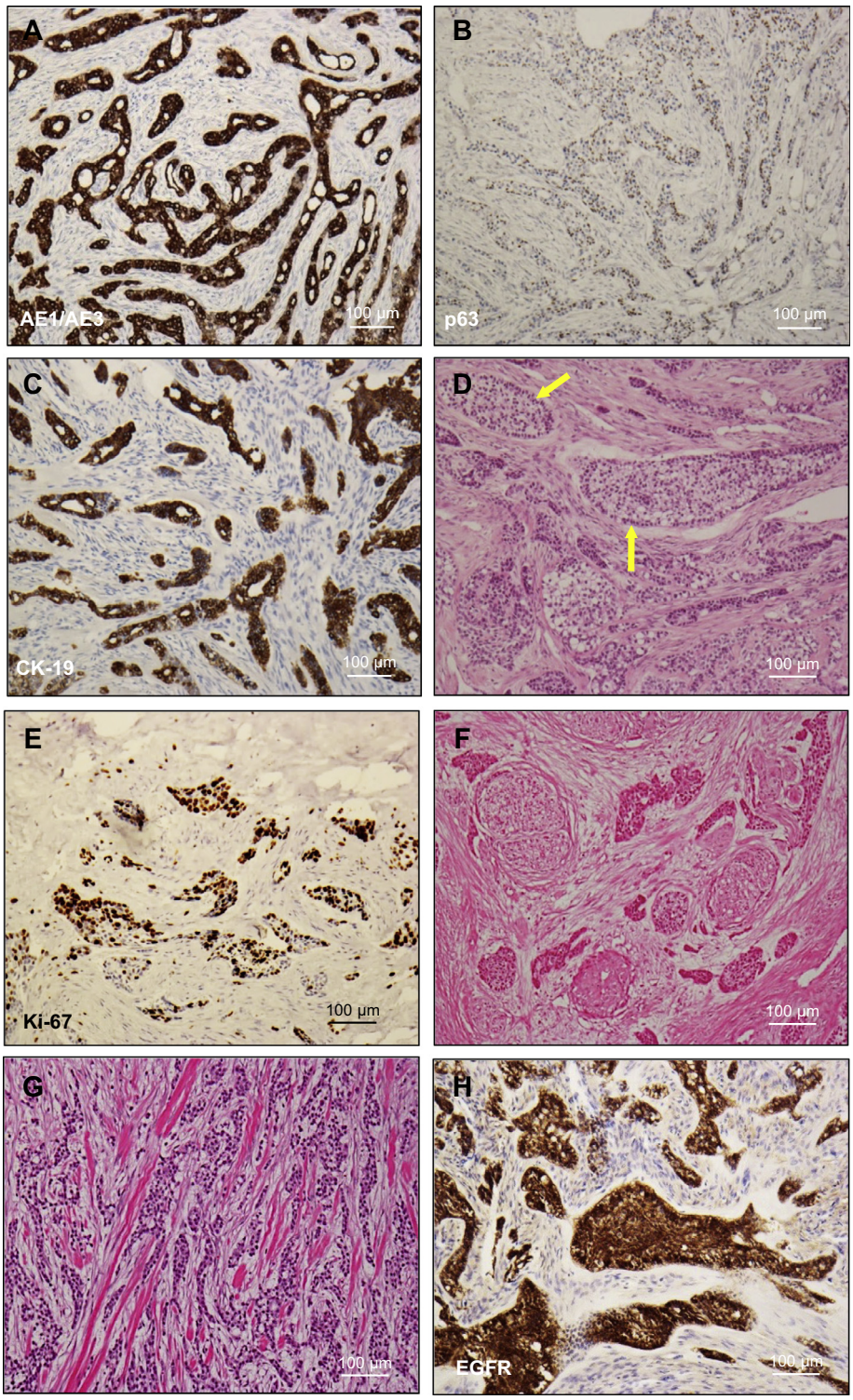

Fig. 2. Histological features in CCOC cases. (A) AE1/AE3 staining. Tumor cells are positive for AE1/AE3. (B) p63 staining. Tumor cells are positive for p63. (C) CK-19 staining. Tumor cells are positive for CK-19. (D) Ameloblastomatous islands with palisaded peripheral cells are observed in the tumor (arrows). (E) Ki-67 staining. The Ki-67 labeling index is over 30%. (F) Neural invasion in the tumor. (G) Histology of metastatic tumor in right scapula. Metastatic lesion in right scapula was found one year after the operation of the primary lesion. (H) Expression of EGFR. Tumor cells are positive for EGFR.

Characterization of the CCOC cell line

We next characterized the CCOC-T cells. First, we examined the growth of the CCOC-T cells. Besides odontogenic carcinoma, MEC and OSCC also arise in the jaw as an intraosseous type. Therefore, we used NCI-H292 (MEC) and HOC313 (OSCC) cells in this experiment. NCI-H292 cells contain the *CRTC1-MAML2* fusion gene, as previously reported (Fig. 5A) [26], and HOC313 cells are highly invasive cancer cells with EMT features [27]. The growth of CCOC-T cells was extremely slow, in comparison with the HOC313 and NCI-H292 cells (Fig. 5B). Next, we examined the invasion activity of these cells. The CCOC-T cells demonstrated signifi-

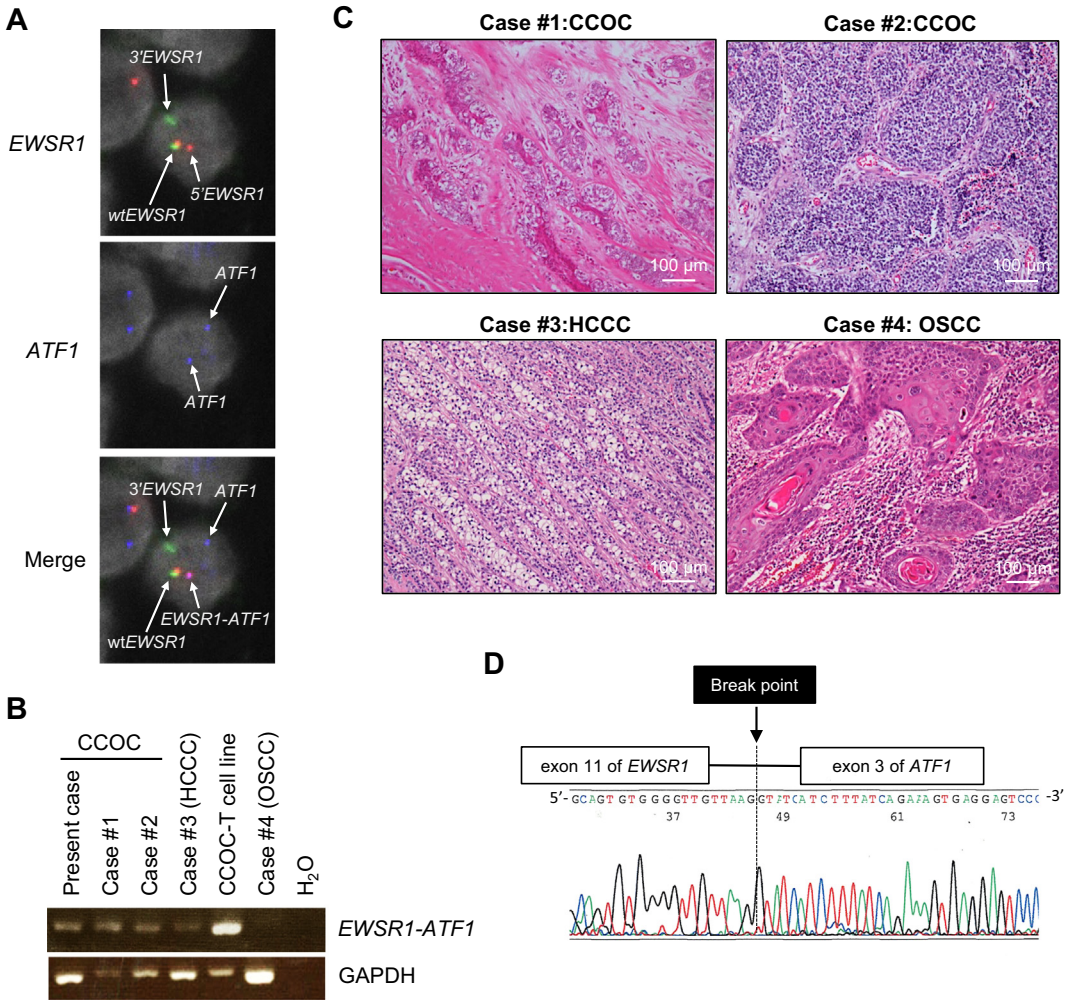

Fig. 3. *EWSR1-ATF1* fusion gene in CCOC cases. (A) *EWSR1-ATF1* rearrangement detected by FISH. Upper left image shows the break-apart FISH for *EWSR1* rearrangement. The majority of tumor cells show a split (separated) signal pattern of one red and one green (arrow; 5′*EWSR1* and 3′*EWSR1*). The intact *EWSR1* is shown by a fused (yellow) signal or closely juxtaposed red and green signals (arrow; wt*EWSR1*). Upper right image shows the ATF1 signal (blue). The red and blue co localized signals indicate the rearrangement involving *EWSR1* and *ATF1* (arrow; *EWSR1-ATF1*). (B) The *EWSR1-ATF1* fusion gene was detected by RT-PCR using FFPE samples. Case #1: CCOC (peripheral); the patient is a male in his 70 s, with a tumor that had arisen in the lower gingiva. Case #2: CCOC; the patient is a male in his 50 s, with a tumor that had arisen in the maxilla. Case #3: HCCC; the patient is a female in her 60 s, with a tumor that had developed in the tongue. Case #4: OSCC; the patient is a male in his 60 s, with a tumor that developed in the oral floor. (C) The histology of Case #1–4 used for the detection of the EWSR1-ATF1 fusion gene. Clinical and histological findings are shown in Supplementary Table 4 and Supplementary Table 5. (D) Sequences of *EWSR1-ATF1* fusion gene in CCOC cases. This image of the RT-PCR product sequencing reveals fusion between *EWSR1* exon 11 and *ATF1* exon 3 (a present case).

cantly higher invasive activity than the NCI-H292 cells (Fig. 5C and D). HOC313 cells revealed the highest invasive activity among all cell types examined.

We examined gene expression in the CCOC-T cells. We confirmed the expression of the *EWSR1-ATF1* fusion gene in the CCOC-T cells (Fig. 5A). Then, we examined the expression of bone-related genes and odotogenic factors including enamel proteins in CCOC-T cells by RT-PCR. CCOC-T cells expressed RUNX2, BSP, COL1, OCN and MSX2 (Fig. 5E). NCI-H292 cells expressed only RUNX2. CCOC-T cells expressed amelogenin, amelotin and KLK4, which are involved in the generation of teeth (Fig. 5F). AM-1 cells were derived from ameloblastoma, which is a typical odontogenic tumor [28]. As expected, AM-1 cells expressed enamel proteins including amelogenin and amelotin (Fig. 5F).

As CCOC-T cells expressed ondontogenic factors, such as amelogenin, amelotin and KLK4, we examined the expression of these molecules by RT-PCR in FFPE samples of CCOC cases (Cases #1 and #2), and a HCCC case (Case #3) as used in Fig. 2B. Although amelotin expression was not observed in all cases (data not shown), amelogenin expression was observed in one of CCOC cases (Case #2) (Fig. 5G). Moreover, KLK4 expression was observed in all CCOC cases but not in HCCC (Fig. 5G). These findings suggest that amelogenin and KLK4 may be used to distinguish between CCOC and HCCC as an odontogenic marker.

Gene expression profile of the CCOC cell line

To know the specific gene expression in CCOC, we compared the gene expression profile of CCOC-T and NCI-H292 cells using a microarray analysis. A total of 326 genes were found to be upregulated by more than fivefold, while 123 genes were downregulated by more than fivefold in CCOC-T cells compared with those of the NCI-H292 cells (Fig. 6A, Supplementary Table 6 and 7). CXCL14, MMP1, MMP2, MMP8, MMP12, ADAM28, FGF9, S100A7, PTCH1, CDH11, SNAI2, and N-cadherin were upregulated in CCOC-T cells. The upregulation of these genes was confirmed by RT-PCR (Fig. 6B). SNAI2 and N-cadherin are well known EMT-promoting factors. Therefore, we examined the expression of EMT-related genes, including SNAI1, E-cadherin and vimentin in CCOC-T cells. While the upregulation of SNAI1 and N-cadherin was observed, E-

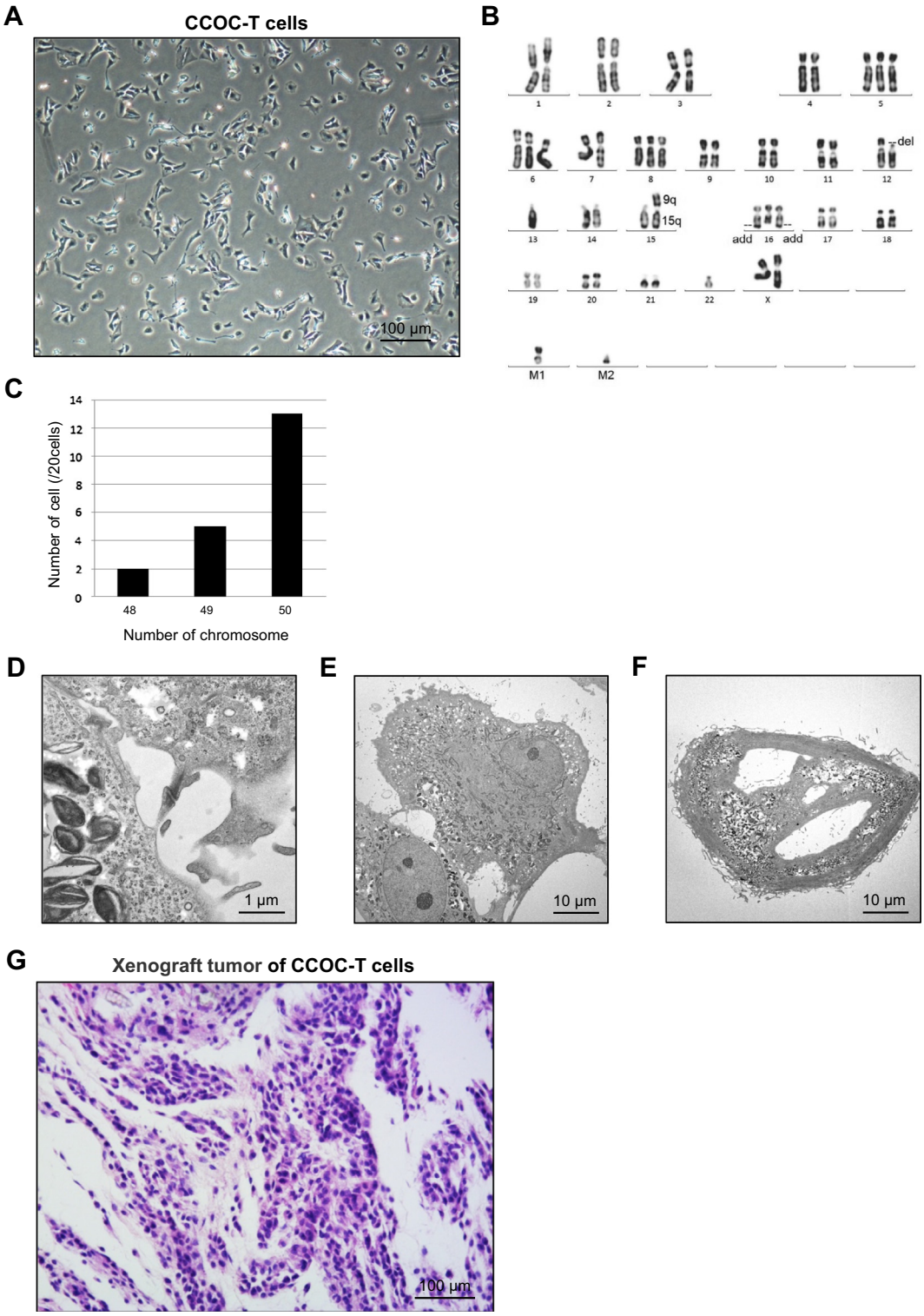

Fig. 4. Establishment and characterization of CCOC-T cells. (A) Phase contrast image of cultured CCOC-T cells that were established from a CCOC case. CCOC-T cells exhibit a polygonal shape. (B) The conventional karyotype of CCOC-T cells. (C) Number of chromosomes of CCOC-T cells. The graph shows the number of chromosomes among 20 CCOC-T cells. (D–F) Figures show the electron microscopic images of the CCOC-T cells. (G) Histology of CCOC-T cells in the xenograft of SCID mice. CCOC-T cells (1×10^6) were injected subcutaneously into multiple sites of male SCID mice.

cadherin downregulation and the upregulation of vimentin were not observed (Fig. 6B). Several invasion and EMT-related genes were also found to be upregulated (GSE84300).

Moreover, we compared the gene expression profile of CCOC-T, NCI-H292, OBA-9 and iOdE. iOdE cells are odontogenic epithelial cells established from epithelial cell rests of Malassez [29], and OBA-9 is immortalized gingival epithelial cells. Among them, 183 genes were found to be commonly upregulated in the cell types of odontogenic origin, CCOC-T and iOdE cells (Fig. 6C and Supplementary Table 8).

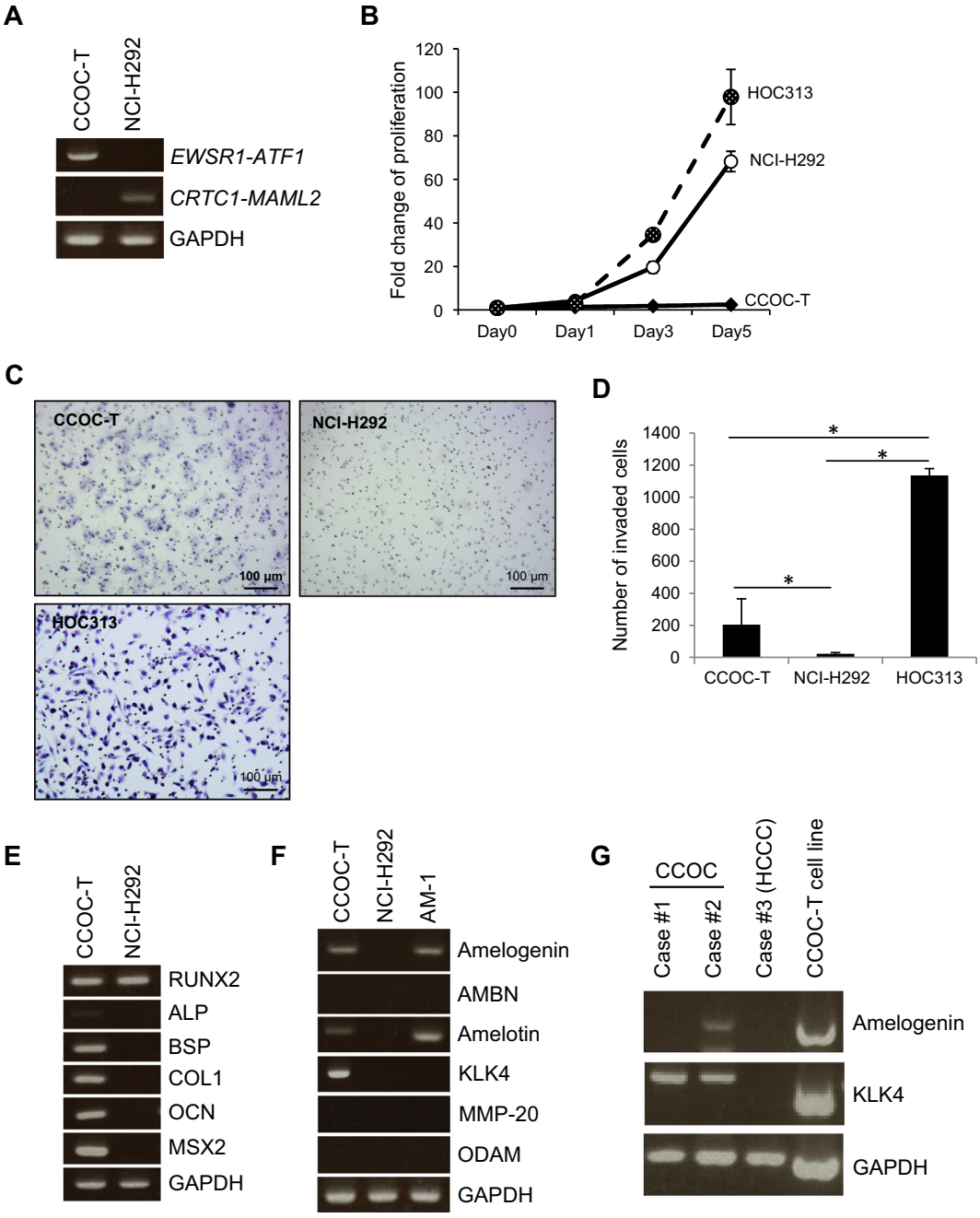

Fig. 5. (A) The *EWSR1-ATF1* fusion gene in CCOC-T cells. *EWSR1-ATF1* and *CRTC1-MAML2* fusion genes were examined by RT-PCR in CCOC-T and NCI-H292 cells. (B) Graph shows the growth of CCOC-T, NCI-H292, and HOC313 cells. Cells were plated into 24-well plates and allowed to adhere for 24 h. Then, trypsinized cells were counted using a cell counter on days 0, 1, 3, and 5. (C) Invasion activity was examined by an *in vitro* invasion assay with CCOC-T, NCI-H292, and HOC313 cells. Figures show the representative area of the penetrated cells. (D) The graph shows the average number of penetrated cells in an *in vitro* invasion assay with CCOC-T, NCI-H292, and HOC313 cells. The bars show the average values and SDs of three independent experiments. $^{*}P < 0.05$. (E) Expression of bone-related genes in CCOC-T cells. Expression of bone-related genes including RUNX2, ALP, BSP, COLI, OCN, and MSX2 was examined by RT-PCR in CCOC-T and NCI-H292 cells. GAPDH was used as a loading control. (F) Expression of odontogenic factors in CCOC-T cells. Expression of odontogenic factors including amelogenein, AMBN, amelotin, KLK4, MMP-20, and ODAM was examined by RT-PCR in CCOC-T, NCI-H292 and AM-1 cells. GAPDH was used as a loading control. (G) Expression of amelogenein, amelotin, and KLK4 in FFPE samples of CCOC and HCCC cases. FFPE samples were used in Fig. 2F. FFPE samples of Case #1 and #2 (CCOC), and Case #3 (HCCC) were used. CCOC-T cells were used as positive control. GAPDH was used as a loading control.

Discussion

Here, the *EWSR1-ATF1* fusion transcript was detected in both CCOC and HCCC cases. Interestingly, exon 11 of *EWSR1* was fused to exon 3 of *ATF1* in all CCOC cases, indicating the same breakpoint found in HCCC [18]. Therefore, the *EWSR1-ATF1* fusion gene as well as histological findings cannot be a distinguishing factor for CCOC and intraosseous HCCC. Cumulating evidences show that primary intraosseous salivary gland tumors are extremely rare. However, two cases of salivary clear cell carcinomas in the mandible which was distinguished from CCOC by the pattern of histological findings were reported [30]. Several hypotheses have been proposed to explain the pathogenesis of intraosseous salivary gland tumors. Although one theory suggests that they may arise from ectopic

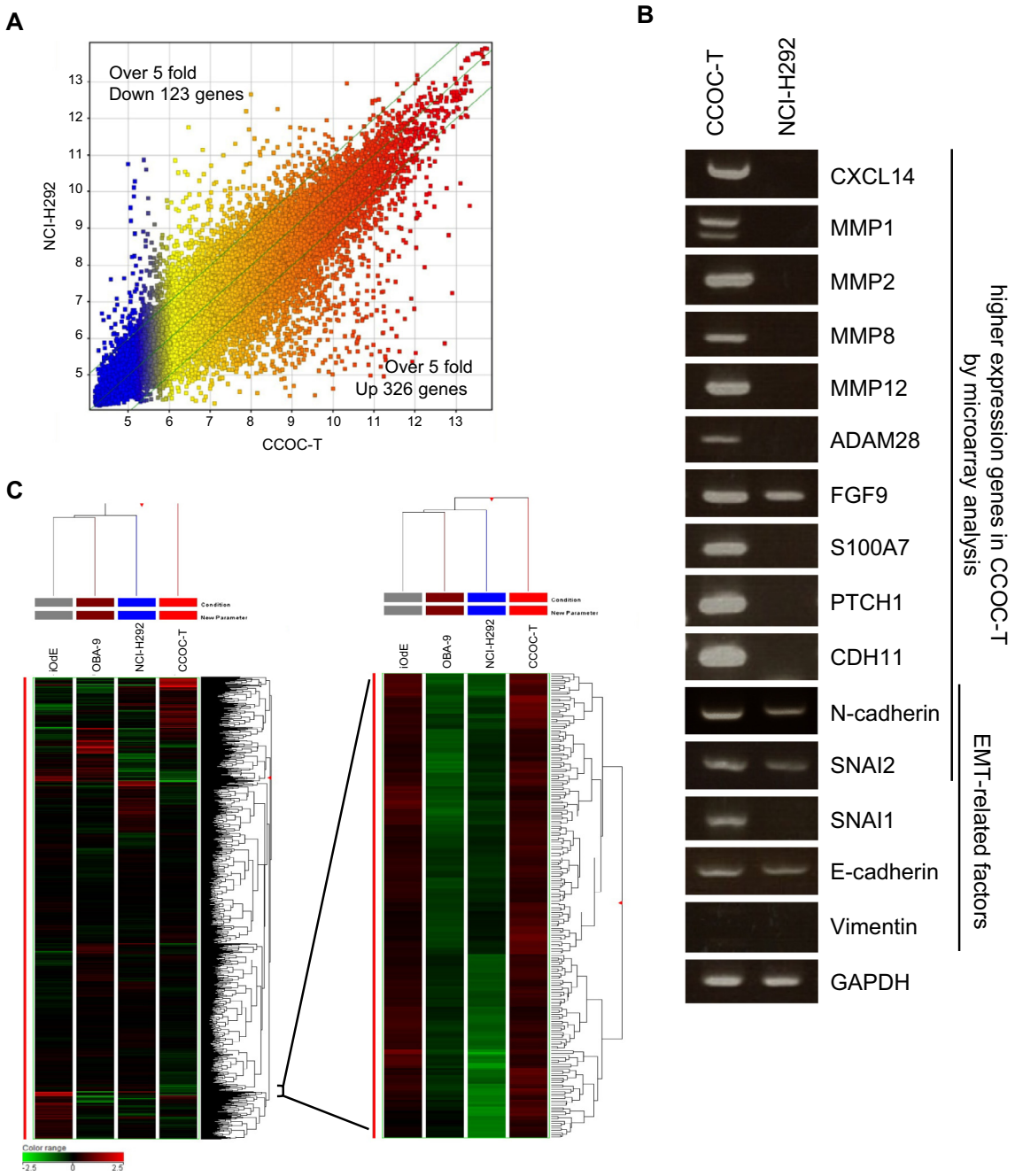

Fig. 6. Gene expression profile of CCOC-T cells. (A) Comparison of the gene expression profiles between CCOC-T cells and NCI-H292 cells by a microarray analysis. Scatter plot of CCOC-T cells (*x* axis) and NCI-H292 cells (*y* axis). The green lines indicate a twofold upregulation or downregulation. (B) Upregulated genes in CCOC-T cells by a microarray analysis (CXCL14, MMP1, MMP2, MMP8, MMP12, ADAM28, FGF9, S100A7, PTCH1, CDH11, N-cadherin and SNAI2) were confirmed by RT-PCR. EMT-related genes, such as SNAI1, E-cadherin, and vimentin were also examined by RT-PCR. GAPDH was used as a loading control. (C) Comparison of the gene expression profile of CCOC-T cells with that of NCI-H292, OBA-9 and iOdE cells. The graph shows the heat map of the gene expression among CCOC-T, NCI-H292, OBA-9 and iOdE cells. Commonly upregulated genes in the cell types of odontogenic origin (CCOC-T and iOdE cells) are highlighted and listed in Supplementary Table 8.

salivary gland tissue that was developmentally entrapped within the jaw, the discovery of ectopic salivary gland tissue is extremely rare in biopsy specimens from the jaw [31]. Therefore, this seems unlikely source for intraosseous salivary gland tumors. The most likely source for intraosseous tumors is odontogenic epithelium. Indeed, mucous-producing cells and glandular structure are frequently found in the lining epithelium of odontogenic cysts. In our case, ameloblastomatous islands with palisaded peripheral cells were observed, suggesting the evidence of an odontogenic origin. These findings suggest that it is difficult to understand that a rare salivary gland carcinoma, HCCC develops in the jaw. Therefore, CCOC represents an "odontogenic analogue" to HCCC. In addition, the expression of odontogenic factors and bone-related genes were observed in CCOC-T cells. Our microarray analyses revealed that 183 genes are commonly upregulated in CCOC-T cells and immortalized odontogenic epithelial cells among other type of cells including gingival epithelial cells and salivary gland tumor cells. This finding may help to identify the specific marker for CCOC. Moreover, we examined the karyotypes of the CCOC-T cells and found that the CCOC-T cells have a translocation (9;15)(q10;q10) and deletion of chromosome 12, suggesting that a specific abnormality may exist in CCOC. However, to identify the specific factors

of CCOC for a differential diagnosis, further experiments are required.

The CCOC-T cells demonstrated enhanced invasiveness and the expression of several MMPs and EMT-promoting factors. This phenotype is consistent with the finding that the primary tumor exhibited malignant behaviors, such as perineural invasion and distant metastasis. Similar to other malignant tumors, EMT may play an important role in the malignant behaviors of CCOC. Interestingly, this tumor strongly expressed EGFR (Fig. 2H). Although there is no report on EGFR expression in odontogenic carcinoma, EGFR inhibitors may be used for the chemotherapy against odontogenic carcinoma including CCOC.

In summary, we established a CCOC cell line (CCOC-T) that exhibited the presence of the *EWSR1-ATF1* fusion gene, odontogenic features, and highly invasive activity. This is the first report regarding the establishment of a CCOC cell line. We believe that CCOC-T cells can be a useful cellular model for understanding the pathogenesis and nature of MOT including CCOC. Moreover, CCOC-T cells may facilitate the discovery of diagnostic makers for the differential diagnosis of this type of cancer.

Conflict of interest statement

All contributing authors declare no conflicts of interest.

Acknowledgements

This study was supported by a Grant-in-Aid from the Ministry of Education, Science, and Culture of Japan. Technical assistance was provided from the Support Center for Advanced Medical Sciences (Tokushima University). The authors thank Mr. Hideaki Horikawa (Tokushima University) for technical assistance and Dr. Ikuko Ogawa (Hiroshima University) for valuable discussion. The authors also thank Dr. Shigehiro Abe and Dr. Naoko Yokomizo (Hiroo hospital) for providing clinical information. In addition, the authors thank Dr. Nobuyuki Kamata (Hiroshima University), Dr. Harada (Iwate Medical University), and Dr. Shinya Murakami (Osaka University) for kindly providing HOC313, AM-1, and OBA-9 cells, respectively.

Appendix A. Supplementary material

Supplementary data associated with this article can be found, in the online version, at http://dx.doi.org/10.1016/j.oraloncology.2017.04.003.

References

[1] Bang G, Koppang HS, Hansen LS, Gilhuus-Moe O, Aksdal E, Persson PG, et al. Clear cell odontogenic carcinoma: report of three cases with pulmonary and lymph node meatastasis. J Oral Pathol Med 1989;18:113–8.
[2] Servato JP, Prieto-Oliveira P, de Faria PR, Loyola AM, Cardoso SV. Odontogenic tumours: 240 cases diagnosed over 31 years at a Brazilian university and a review of international literature. Int J Oral Maxillofac Surg 2013;42:288–93.
[3] Fan J, Kubota E, Imamura H, Shimokama T, Tokunaga O, Katsuki T, et al. Clear cell odontogenic carcinoma: a case report with massive invasion of neighboring organs and lymph node metastasis. Oral Surg Oral Med Oral Pathol 1992;74:768–75.
[4] Milles M, Doyle J, Mesa M, Raz S. Clear cell odontogenic carcinoma with lymph node metastasis. Oral Surg Oral Med Oral Pathol 1993;76:82–9.
[5] Li TJ, Yu SF, Gao Y, Wang EB. Clear cell odontogenic carcinoma: a clinicopathologic and immunocytochemical study of 5 cases. Arch Pathol Lab Med 2001;125:1566–71.
[6] Zhang J, Liu L, Pan J, Tian X, Tan J, Zhou J, et al. Clear cell odontogenic carcinoma: report of 6 cases and review of the literature. Med Oncol 2011;28:S626–33.
[7] Yazici ZM, Mete O, Elmali Z, Sayin I, Yilmazer R, Kayhan FT. Clear cell odontogenic carcinoma of the maxilla. Acta Med (Hradec Kralove) 2011;54:122–4.
[8] Infante-Cossio P, Torres-Carranza E, Gonzalez-Perez LM, Gonzalez-Cardero E, Sanchez-Gallego F. Atypical presentation of clear cell odontogenic carcinoma. J Craniofac Surg 2012;23:e466–8.
[9] Swain N, Dhariwal R, Ray JG. Clear cell odontogenic carcinoma of maxilla: a case report and mini review. J Oral Maxillofac Pathol 2013;17:89–94.
[10] Kalsi AS, Williams SP, Shah KA, Fasanmade A. Clear cell odontogenic carcinoma: a rare neoplasm of the maxillary bone. J Oral Maxillofac Surg 2014;72:935–8.
[11] Yancoskie AE, Sreekantaiah C, Jacob J, Rosenberg A, Edelman M, Antonescu CR, et al. EWSR1 and ATF1 rearrangements in clear cell odontogenic carcinoma: presentation of a case. Oral Surg Oral Med Oral Pathol Oral Radiol 2014;118:e115–8.
[12] Krishnamoorthy R, Ravi Kumar AS, Batstone M. FDG-PET/CT in staging of clear cell odontogenic carcinoma. Int J Oral Maxillofac Surg 2014;43:1326–9.
[13] Kim M, Cho E, Kim JY, Kim HS, Nam W. Clear cell odontogenic carcinoma mimicking a cystic lesion: a case of misdiagnosis. J Korean Assoc Oral Maxillofac Surg 2014;40:199–203.
[14] Kwon IJ, Kim SM, Amponsah EK, Myoung H, Lee JH, Lee SK. Mandibular clear cell odontogenic carcinoma. World J Surg Oncol 2015;13:284.
[15] Ban G, Koppang H. Odontogenic clear cell carcinoma. In: Barnes L, Eveson JW, Reichart P, Sidransky D, editors. World health organization classification of tumours. Pathology and genetics of head and neck tumours. Lyon: IARC Press; 2005. p. 292.
[16] Bilodeau EA, Weinreb I, Antonescu CR, Zhang L, Dacic S, Muller S, et al. Clear cell odontogenic carcinomas show EWSR1 rearrangements: a novel finding and a biologic link to salivary clear cell carcinomas. Am J Surg Pathol 2013;37:1001–5.
[17] Tanguay J, Weinreb I. What the EWSR1-ATF1 fusion has taught us about hyalinizing clear cell carcinoma. Head Neck Pathol 2013;7:28–34.
[18] Antonescu CR, Katabi N, Zhang L, Sung YS, Seethala RR, Jordan RC, et al. EWSR1-ATF1 fusion is a novel and consistent finding in hyalinizing clear-cell carcinoma of salivary gland. Genes Chromosomes Cancer 2011;50:559–70.
[19] Milchgrub S, Gnepp DR, Vuitch F, Delgado R, Albores-Saavedra J. Hyalinizing clear cell carcinoma of salivary gland. Am J Surg Pathol 1994;18:74–82.
[20] Bilodeau EA, Hoschar AP, Bames EL, Hunt JL, Seethala RR. Clear cell carcinoma and clear cell odontogenic carcinoma: a comparative clinicopathologic and immunohistochemical study. Head Neck Pathol 2011;5:101–7.
[21] Iezzi G, Rubini C, Fioroni M, Piattelli A. Clear cell odontogenic carcinoma. Oral Oncol 2002;38:209–13.
[22] Mosqueda-Taylor A, Meneses-Garcia A, Ruiz-Godoy Rivera LM, de Lourdes Suárez-Roa M. Clear cell odontogenic carcinoma of the mandible. J Oral Pathol Med 2002;31:439–41.
[23] Piattelli A, Sesenna E, Trisi P. Clear cell odontogenic carcinoma. Report of a case with lymph node and pulmonary metastases. Eur J Cancer B Oral Oncol 1994;30B:278–80.
[24] Brandwein M, Said-Al-Naief N, Gordon R, Urken M. Clear cell odontogenic carcinoma: report of a case and analysis of the literature. Arch Otolaryngol Head Neck Surg 2002;128:1089–95.
[25] Weinreb I. Hyalinizing clear cell carcinoma of salivary gland: a review and update. Head Neck Pathol 2013;7:S20–9.
[26] Amelio AL, Fallahi M, Schaub FX, Zhang M, Lawani MB, Alperstein AS, et al. CRTC1/MAML2 gain-of-function interactions with MYC create a gene signature predictive of cancers with CREB-MYC involvement. Proc Natl Acad Sci USA 2014;111:E3260–8.
[27] Nguyen PT, Kudo Y, Yoshida M, Kamata N, Ogawa I, Takata T. N-cadherin expression is involved in malignant behavior of head and neck cancer in relation to epithelial-mesenchymal transition. Histol Histopathol 2011;26:147–56.
[28] Harada H, Mitsuyasu T, Nakamura N, Higuchi Y, Toyoshima K, Taniguchi A, et al. Establishment of ameloblastoma cell line, AM-1. J Oral Pathol Med 1998;27:207–12.
[29] Tsunematsu T, Fujiwara N, Yoshida M, Takayama Y, Kujiraoka S, Qi G, et al. Human odontogenic epithelial cells derived from epithelial rests of Malassez possesses stem cell properties. Lab Invest 2016;96:1063–75.
[30] Berho M, Huvos AG. Central hyalinizing clear cell carcinoma of the mandible and the maxilla a clinicopathologic study of two cases with an analysis of the literature. Hum Pathol 1999;30:101–5.
[31] Bouquot JE, Gnepp DR, Dardick I, Hietanen JH. Intraosseous salivary tissue: jawbone examples of choristomas, hamartomas, embryonic rests, and inflammatory entrapment: another histogenetic source for intraosseous adenocarcinoma. Oral Surg Oral Med Oral Pathol Oral Radiol Endod 2000;90:205–17.